Contents

Chapter 1

Plasmas in Penning Traps

This chapter introduces the reader to the physics of plasmas in Penning traps. After a brief discussion of what constitutes a classical plasma, and a description of Debye shielding, the basic equilibrium properties of non-neutral plasmas in Penning traps are explained. Plasma rotation, the Brillouin limit, diamagnetic effects, the confined thermal equilibrium state, and constants of the motion are discussed.

1. What is a Plasma?

A plasma is a state of matter with properties quite distinct from the solid, liquid, or gas phases that you are more familiar with from your physics classes. In fact, plasma is often referred to as the "fourth state of matter".[1] In the following two chapters, we will consider a few of the properties of the plasma state, particularly as they pertain to confined plasmas in Penning traps.

A plasma is a collection of charged particles moving freely under the influence of external force fields as well as self-generated electric and/or magnetic fields. In a plasma, these self-generated fields are sufficiently large to significantly affect the particle dynamics. Plasmas are often produced by heating a neutral gas until a significant fraction of the particles become ionized through collisional processes; however, low temperature plasmas also exist in both nature and the laboratory. In fact, plasma temperatures can be sufficiently low, and/or densities can be sufficiently high, that quantum phenomena (such as Pauli exclusion[5] or quantized energies[6,7]) play an important role in the plasma equilibrium and dynamics. However, in these chapters, I will concentrate on those regimes where the plasma state is well-described by classical mechanics. I will also neglect relativistic effects, assuming particle velocities are small compared to the speed of light (an excellent approximation in most Penning trap experiments).

Also, plasmas are not always charge-neutral – particularly in Penning trap experiments, the number of negative charges does not always balance the number of positive charges. Such plasmas are called "non-neutral".[8]

Below, I consider in more detail the requirements for a system to be in the plasma state.

1.1. *The Debye length*

The Debye length λ_D is a fundamental length scale in plasmas. It is the length over which static electric fields are "screened out" in an unmagnetized thermal classical plasma. To understand what this means, consider the following simple plasma configuration: a parallel plate capacitor is introduced into a neutral plasma consisting of electrons and singly-charged ions with equal densities n_0 and charges $-e$ and $+e$ respectively(Fig. 1). I assume that this plasma has a well-defined temperature T, and I apply a potential V to the left capacitor electrode (at position $x = 0$) and ground the right electrode (which is at position $x = L$). If there were no plasma present, this would produce a potential be-

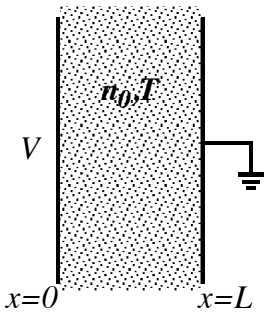

Fig. 1.: A neutral plasma between the plates of a capacitor shields out the applied electric field.

tween the electrodes given by

$$\phi(x) = V(1 - x/L), \tag{1}$$

which corresponds to a uniform electric field $E = V/L$ between the plates. However, the plasma *significantly affects* this potential, reducing the electric field to nearly zero after a "sheath" layer whose width is given by the Debye length. This is what is meant by "plasma screening". To analyze this screening phenomenon, I assume for simplicity that the plasma is in a thermal equilibrium state at temperature T. (Here I should note, in the interests of full disclo-

sure, that plasmas in contact with conducting plates as shown in the figure are typically not in thermal equilibrium because the plates draw current from the plasma, are not at the same temperature as the plasma, and may react chemically with the plasma; and consequently the plasma screening that occurs is much more complicated than the simple model put forward here. The conducting plates I am using are *magic plates* that can be heated to the same temperature as the plasma without vaporizing, and also somehow neither emit nor absorb electrons or ions.) The thermal equilibrium model implies that the electron and ion densities n_e and n_i are described by Boltzmann distributions:[9]

$$n_e(x) = n_0 \exp(e\phi(x)/T) \tag{2}$$

$$n_i(x) = n_0 \exp(-e\phi(x)/T) \tag{3}$$

That is, the electrons are attracted to the plate at positive potential, increasing their density there, while the ions are repelled from that region; and the zero of potential is defined to be in the region where the plasma achieves density n_0. (Note that in these chapters temperature is regarded as having units of energy, and therefore the Boltzmann constant k_B is unnecessary. Boltzmann, the founder of statistical mechanics and one of the great scientific innovators of the late 19th and early 20th centuries, deserves to have a better constant named after him!)

The charge distribution arising from Eqs. (2) and (3) has an appreciable effect on the electrostatic potential ϕ. The potential is determined from the Poisson equation,

$$\begin{aligned} \frac{d^2\phi}{dx^2} &= \frac{e}{\varepsilon_0}[n_e(x) - n_i(x)] \\ &= \frac{n_0 e}{\varepsilon_0}\left[\exp(e\phi/T) - \exp(-e\phi/T)\right]. \end{aligned} \tag{4}$$

Equation (4) can be solved subject to the boundary conditions that $\phi(0) = V$ and $\phi(L) = 0$. For simplicity, I will facilitate this solution by linearizing the equation in ϕ, assuming that $|e\phi/T| \ll 1$:

$$\frac{d^2\phi}{dx^2} = 2\frac{n_0 e^2}{\varepsilon_0 T}\phi. \tag{5}$$

The factor of two that appears on the right-hand side arises from the shielding effect of the two species considered here, i.e. electrons and singly-charged ions. If more species were added, with arbitrary charges, this factor would be modified.[10]

The solution to Eq. (5) that matches the required boundary conditions is

$$\phi(x) = V\frac{\exp(-\sqrt{2}x/\lambda_D) - \exp(\sqrt{2}(x-2L)/\lambda_D)}{1-\exp(-2\sqrt{2}L/\lambda_D)} \tag{6}$$

$$\simeq V\exp(-\sqrt{2}x/\lambda_D),\ L \gg \lambda_{D,} \tag{7}$$

where the Debye length λ_D is defined in terms of the equilibrium density and temperature as

$$\lambda_D \equiv \sqrt{\frac{\varepsilon_0 T}{n_0 e^2}} \tag{8}$$

$$= 743\ \mathrm{m}\sqrt{\frac{T(\mathrm{eV})}{n_0(\mathrm{m}^{-3})}}.$$

Equation (7) implies that the electric field in the plasma is *exponentially suppressed*. The positively charged capacitor plate attracts plasma electrons and repels ions. After a sheath region which is a few Debye-lengths thick, the electric field is nearly zero: it has been screened out by the plasma.

1.2. *Requirements for the plasma state*

These considerations lead us to our first requirement that a system be in the plasma state: in order for the plasma to significantly affect the potential, the Debye length must be small compared to the system size; otherwise the screening effect of the plasma is negligible:

$$\lambda_D \ll L \text{ in the plasma state.} \tag{9}$$

If this requirement is not met and the Debye length is larger than L, one can see from Eq. (6) that the potential returns to the vacuum form, Eq. (1).

A second requirement follows from certain assumptions in the preceding analysis. In describing the ions and electron densities with Eqs (2) and (3), I have have implicitly treated them as continuous fluids. This is only a good approximation provided that the density varies slowly on the scale of the mean inter-particle spacing $a \equiv n_0^{-1/3}$. Since the density varies on the scale of the Debye length, it is necessary that $\lambda_D \gg n_0^{-1/3}$. This inequality is often rearranged to read

$$n_0\lambda_D^3 \gg 1 \text{ in the plasma state.} \tag{10}$$

The dimensionless quantity $n_0\lambda_D^3$, the number of charges in a "Debye-sphere", is called the plasma parameter.[3] Some further intuition regarding this expres-

sion can be found by rewriting Eq. (10) using Eq. (8):

$$n_0\lambda_D^3 = \left[\frac{T}{e^2/\varepsilon_0 a}\right]^{3/2}, \tag{11}$$

which is the ratio of the mean kinetic energy of a particle, T, to the mean interaction potential energy $e^2/\varepsilon_0 a$ between nearest-neighbors. This ratio must be large in the plasma state, so the plasma is a *nearly ideal gas* of weakly-interacting charges. However, this does not mean that one can ignore the *collective* interaction of many charges with one-another, which gives rise to large potentials sufficient to screen out applied fields or produce plasma waves (as discussed in the next chapter).

Plasmas for which the plasma parameter is of order unity or even smaller than unity are referred to as non-ideal plasmas, or strongly-coupled plasmas.[10] Since the kinetic energy per particle is on the same order as, or even smaller than, the interaction energy, these plasmas might be better thought of as liquids or possibly even solids. The properties of non ideal plasmas, and their study in Penning traps, will be the subject of other chapters in this course. Here, I will focus on "standard-issue" nearly-ideal plasmas.

Question (1 a). If the capacitor plates are 1cm apart and the plasma temperature is 10eV, what density is required in order for there to be at least 10 Debye lengths between the plates?

Question (1b): The Orion Nebula is a roughly spherical mass of almost fully-ionized Hydrogen with a radius of about 20 light years and a mean charged particle density of roughly $n_0 = 10^8 \mathrm{m}^{-3}$. If it were in thermal equilibrium (it is not – portions of it are far from equilibrium!) with a temperature of $T = 100$ eV, what would its Debye length be? Under these assumptions, would you classify the Orion Nebula as a plasma?

2. Non-neutral plasmas in Penning traps

A non-neutral plasma is a plasma in which the number of negative and positive charge species are unequal.[8] Most plasmas are at least slightly non-neutral; such plasmas are often referred to as "quasi-neutral". In this chapter I will be concerned with fully-unneutralized plasmas consisting only of species with the same sign of charge. Many such plasmas that have been created and studied experimentally: pure electron plasmas;[11] mixed electron and antiproton plasmas;[12] mixed positron and positive ion plasmas;[13] negative ion plasmas.[14] In these experiments, the plasmas can satisfy relations (9) and(10), and therefore exhibit strong Debye shielding of externally applied potentials.

These fully-unneutralized non-neutral plasmas are studied for a number of reasons. First and possibly foremost, they have exceptional confinement properties: they can be confined in a rotating thermal equilibrium state away from surrounding walls, in an electromagnetic bottle called a Penning trap[15] that uses only static electric and magnetic fields.[16] (We will see that the same cannot be said of neutral plasmas!) The existence of a confined thermal equilibrium state implies that the plasmas are inherently low noise and reproducible, since there is no free energy available to drive the kinds of instabilities that plague neutral plasma devices.

The range of densities that can be accessed by these non-neutral plasmas is smaller than for neutral plasmas, and it depends on the strength of the confining magnetic field. Densities are typically less than $10^{16}\mathrm{m}^{-3}$ for pure electron plasmas, and even less for ions. However, the temperatures in experiments can range over many orders of magnitude from 1 mK up to 10 eV or more, allowing a range of phenomena to be studied. For example, if a neutral plasma were cooled to 1 mK, it would immediately recombine to a neutral gas. However, in a fully-unneutralized plasma, there is no oppositely charged species with which to recombine. Furthermore, at such low temperatures the plasma parameter is much smaller than unity and the plasma is strongly-coupled, exhibiting liquid and even crystalline phases. This interesting behavior will be discussed by other speakers.

Here, I will first consider the confinement characteristics of a non-neutral plasma in a Penning trap.

2.1. *The Penning-Malmberg Trap*

Figure 2 shows a schematic of a Penning-Malmberg trap (a Penning trap with cylindrical electrodes[11]). Voltages are applied to the end electrodes in order to produce a potential well in the axial direction that confines charges with a given sign of charge (assumed positive in the case of Fig. 2). Confinement against radial plasma expansion is provided by the magnetic field $\mathbf{B} = B\hat{z}$, directed along the axis of symmetry of the trap. The plasma rotates around the axis of symmetry, and the rotational velocity provides an inward-directed $\mathbf{v}\times\mathbf{B}$ force that balances the outward-directed radial electric force from the unneutralized plasma charge.

To analyze this plasma configuration in more detail, I will apply fluid equations of motion.For a single species plasma consisting of charges with mass m, charge q, and density n, the momentum equation for the plasma's fluid velocity $\mathbf{u}$ is[4,20]

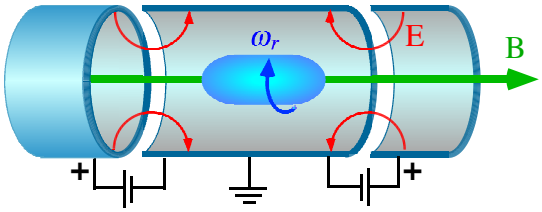

Fig. 2.: Cutaway view of the cylindrical electrodes showing a positively-charged non-neutral plasma confined in a Penning-Malmberg trap.

$$mn\left(\frac{\partial \mathbf{u}}{\partial t}+\mathbf{u}\cdot\nabla\mathbf{u}\right)=qn\left(-\nabla\phi+\mathbf{u}\times\mathbf{B}\right)-\nabla p, \tag{12}$$

where p is the plasma's thermal pressure. In what follows, q is a signed quantity; it can be either positive or negative.

Throughout the rest of this chapter, I will also assume that the plasma has achieved a confined thermal equilibrium state. In this thermal equilibrium state the plasma rotates, with a the time-independent fluid velocity given by the expression $\mathbf{u}(r)=-\omega_r r\widehat{\theta}$, where cylindrical coordinates are being employed, and ω_r is the rotation frequency (in radians per second). The negative sign in this expression reflects the fact that a positively charged plasma will rotate in the $-\widehat{\theta}$ direction; thus, for positive plasmas ω_r is a positive quantity; but for a negative plasma ω_r is less than zero.

In thermal equilibrium the plasma rotation frequency is constant in time and uniform in space; if it were nonuniform, viscous effects would cause any such velocity shears to relax until the plasma rotates rigidly.

Also, in thermal equilibrium, the plasma pressure p is related to density and temperature T through the ideal gas law (since the plasma is a nearly ideal gas): $p=nT$, where T is time-independent and uniform in space (note that throughout the chapter I measure T in units of energy). If the temperature were not uniform, it would relax through thermal conduction.

First, let us consider the z-component of Eq. (12):

$$0=-qn\frac{\partial\phi}{\partial z}-T\frac{\partial n}{\partial z}. \tag{13}$$

Consider first the "zero-temperature" limit (i.e. the regime where temperatures are small enough so that the second "pressure" term on the rhs can be neglected). In this limit, the equation implies that wherever the density is nonzero, the z-component of the electric field is zero. This is the Debye-shielding phenomenon discussed in the previous section, in the limit of zero Debye length. More generally, at finite T, the z-electric field is shielded out inside the plasma within a few Debye-lengths of the plasma surface.

For finite T, Eq. (13) can be integrated to yield the Boltzmann-like relation

$$n(r,z) = N(r)\exp[-q\phi(r,z)/T], \tag{14}$$

for any function $N(r)$. This function is determined by the radial component of the momentum equation, which is given below:

$$-mn\omega_r^2 r = -qn\left(\frac{\partial\phi}{\partial r} + B\omega_r r\right) - T\frac{\partial n}{\partial r}. \tag{15}$$

The term on the lhs is the centripetal force density associated with rigid rotation arising from the $\mathbf{u}\cdot\nabla\mathbf{u}$ term in Eq. (12). This force density must be in balance with the radial forces from the electric potential, rotation through the magnetic field, and pressure.

2.2. *Plasma Density*

By substituting Eq. (14) for the density into Eq. (15), some cancelations occur and the result is a simple differential equation for $N(r)$:

$$T\frac{\partial N}{\partial r} = -m\omega_r(\Omega_c - \omega_r)r\,N, \tag{16}$$

where $\Omega_c = qB/m$ is the cyclotron frequency [a positive(negative) quantity for positive(negative) charges]. This equation can be integrated and the result combined with Eq. (14) to yield the following expression for the plasma density in thermal equilibrium:

$$n(r,z) = C\exp\{-q[\phi(r,z) + \phi_{eff}(r)]/T\}, \tag{17}$$

where C is a constant of integration and where the *effective potential* ϕ_{eff} is defined as

$$q\phi_{eff}(r) \equiv \tfrac{1}{2}m\omega_r(\Omega_c - \omega_r)r^2. \tag{18}$$

This quadratic potential provides radial confinement due to rotation: provided that $\omega_r(\Omega_c - \omega_r) > 0$, the effective potential becomes large at large r, dominating over ϕ and forcing the density to become exponentially small (see Eq. (17)). This inequality requires that $0 < \omega_r/\Omega_c < 1$ for confinement. If ω_r/Ω_c were

greater than unity, the deconfining centrifugal force would win out over the confining $\mathbf{v}\times\mathbf{B}$ force.

In order to close the system and solve for the density, one must determine the potential $\phi(r,z)$. This is done solving the Poisson equation with boundary conditions given by the voltages on the cylindrical electrodes, and with density in terms of ϕ given by Eq. (17) :

$$\nabla^2\phi(r,z) = -qn(r,z)/\varepsilon_0. \tag{19}$$

2.3. *The uniform background charge, the Brillouin limit, and fluid drifts*

There is another useful way to think about the effective potential that aids in understanding the solution to Eq. (19). A quadratic radial potential can also be produced by a cylinder of uniform density negative background charge. Using the Poisson equation it is easy to show that the background density n_0 required to create an effective potential given by Eq. (18) is

$$n_0 = 2\frac{m\varepsilon_0}{q^2}\omega_r(\Omega_c-\omega_r). \tag{20}$$

Thus, one can think of the plasma as being radially confined by this cylindrical neutralizing background charge rather than by rotation through a magnetic field; Eq. (16) for the plasma density would be the same either way. Intuitively, one would then expect that, in equilibrium, the plasma matches its density to the negative background charge density, out to some surface of revolution (determined by the total number of particles, the uniform background density n_0, and the voltages applied to the electrodes) where the supply of plasma charge is exhausted and the density approaches zero.[17] In fact, this is just what the solution to Eqs. (19) and(17) show.[19] At the plasma surface the density falls from n_0 to zero on the scale of a few Debye lengths. Thus, within the plasma (i.e. several Debye lengths away from the edge) the density is uniform and given by Eq. (20), provided that the plasma length and radius are both large compared to the Debye length.

Experiments with nearly-uniform density plasmas are often carried out in a regime where $\omega_r/\Omega_c \ll 1$. In this regime one can easily solve Eq. (20) for the rotation frequency in terms of the plasma density by approximating $\Omega_c-\omega_r \approx \Omega_c$ in Eq. (20), yielding

$$\omega_r \approx \frac{qn_0}{2\varepsilon_0 B}. \tag{21}$$

This equation shows that, at low densities, increasing the density requires a higher rotation frequency in order to produce a larger $\mathbf{v}\times\mathbf{B}$ confining force

that balances the larger electrostatic repulsion. However, Eq. (20) shows that this balance only works up to a point: if the rotation rate is raised too high, centrifugal force begins to win out over the $\mathbf{v}\times\mathbf{B}$ force, and the density actually decreases as the rotation rate increases. For this reason there is a maximum possible plasma density that can be confined in thermal equilibrium, called the *Brillouin limit,*.[18] The Brillouin limit follows from the form of Eq. (20), which implies that as one varies ω_r the density reaches a maximum value n_B when $\omega_r = \Omega_c/2$, given by

$$\begin{aligned} n_B &= \frac{m\varepsilon_0\Omega_c^2}{2q^2} \\ &= \frac{B^2}{2\mu_0 mc^2}, \end{aligned} \tag{22}$$

where I have used the identity $\varepsilon_0\mu_0 = 1/c^2$. Equation (22) shows that the plasma's maximum rest energy density $n_B mc^2$ is equal to the magnetic energy $B^2/2\mu_0$. This implies a fairly low maximum density for magnetic fields currently available in the laboratory. For electrons in a 1 Tesla field, the density at the Brillouin limit is 4.8×10^{18} m^{-3}.

Another useful equation relating the plasma rotation frequency to the plasma density and potential is found by dividing Eq. (15) by $mnr\Omega_c$ and rearranging terms so that the equation reads

$$\omega_r = -\frac{1}{Br}\frac{\partial\phi}{\partial r} - \frac{T}{qBrn}\frac{\partial n}{\partial r} + \frac{\omega_r^2}{\Omega_c}. \tag{23}$$

Thus, the uniform rotation frequency is a sum of three terms, which correspond to three different effects. The first term on the rhs of Eq. (23) can be recognized as the rotation frequency arising from the $\mathbf{E}\times\mathbf{B}$ drift discussed in other chapters. At low rotation frequencies and in a cold plasma, this term dominates and is responsible for the rotation frequency given by Eq. (21).

The last term in Eq. (23) is a correction to $\mathbf{E}\times\mathbf{B}$ drift caused by the centrifugal force from rotation, which produces an extra $\mathbf{F}\times\mathbf{B}$ drift. The middle term, proportional to the temperature, is a rotation of the plasma induced by the *diamagnetic drift*. This drift is caused by cyclotron motion in a nonuniform plasma. Figure 3 shows a close-up of a section of the plasma edge. The magnetic field is out of the page. In this figure the $\mathbf{E}\times\mathbf{B}$ and centrifugal drifts are neglected, so charges simply undergo circular cyclotron motion. However, the existence of a density gradient implies that there are more particles on the left than on the right and consequently at any radius the particle cyclotron motion causes a net fluid velocity downward (assuming positive charges), as depicted in the figure.

The diamagnetic fluid velocity is closely connected to the diamagnetic currents associated with diamagnetic materials. In these materials, an applied magnetic field induces magnetic dipole moments in particles making up the material, and these dipoles act to produce a surface current that creates a magnetic field opposed to the applied field. In the plasma, cyclotron motion due to the applied magnetic field produces current loops (see Fig. 3) that also have magnetic moments, and there is therefore also a net surface current. Furthermore, one can show that this surface current creates a magnetic field that opposes the applied magnetic field; it is, truly, a *diamagnetic* current. This diamagnetic contribution to the magnetic field has been neglected (as have the contributions from the $\mathbf{E} \times \mathbf{B}$ and centrifugal drifts) because these self-generated fields are weak in most experiments (see Question 2 at the end of the chapter).

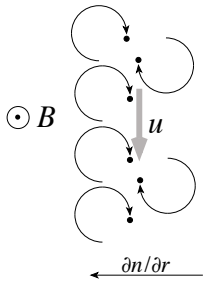

Fig. 3.: The diamagnetic drift produces a contribution to the fluid velocity **u** at the plasma edge.

2.4. *The velocity distribution, canonical momentum, and the vortex frequency*

In thermal equilibrium the full distribution function $f(\mathbf{r},\mathbf{v})$ is a product of the equilibrium density given by Eq. (17) and a Maxwellian velocity distribution, shifted by the fluid rotation velocity $\mathbf{u} = -\omega_r r\widehat{\theta}$:

$$f(\mathbf{r},\mathbf{v}) = \frac{C}{(2\pi T/m)^{3/2}} e^{-q(\phi+\phi_{eff})/T} e^{-m(\mathbf{v}+\omega_r r\widehat{\theta})^2/2T} \tag{24}$$

$$= \frac{C}{(2\pi T/m)^{3/2}} e^{-H_r/T}, \tag{25}$$

where

$$H_r \equiv \frac{m}{2}(\mathbf{v}+\omega_r r\widehat{\theta})^2 + q\phi(r,z) + q\phi_{eff}(r). \tag{26}$$

The function H_r is the particle energy as seen in a frame rotating with the plasma: the particle velocity as seen in the rotating frame is $\mathbf{v}+\omega_r r\widehat{\theta}$, and the kinetic energy in this frame is proportional to the square of this apparent velocity. Also, this velocity is, on average, zero: the plasma is stationary when seen in the rotating frame (i.e. the mean fluid velocity is zero in this frame) . The frame is not inertial and consequently there is an effective potential $e\phi_{eff}(r)$ due to centrifugal and Lorentz forces arising from rotation. When viewed in the rotating frame, the distribution function for this apparently stationary equilibrium plasma has the expected Boltzmann form, Eq. (25).[16]

It is useful to rewrite the particle kinetic energy in terms of the *canonical momentum* $\mathbf{p} = m\mathbf{v} + q\mathbf{A}$, where $\mathbf{A}$ is the vector potential. For a uniform magnetic field $\mathbf{B} = B\hat{z}$, the vector potential can be expressed as $\mathbf{A} = Br\widehat{\theta}/2$. This implies one may write the particle velocity $\mathbf{v}$ in terms of $\mathbf{p}$ as

$$\mathbf{v} = \frac{\mathbf{p}}{m} - \frac{1}{2}\Omega_c r\widehat{\theta}.$$

Applying this expression for the velocity to Eq. (26) yields

$$H_r = \frac{m}{2}(\mathbf{p} - m\Omega_v r\widehat{\theta}/2)^2 + q\phi(r,z) + q\phi_{eff}(r), \tag{27}$$

where I have introduced the vortex frequency Ω_v, defined as

$$\Omega_v \equiv \Omega_c - 2\omega_r. \tag{28}$$

The vortex frequency is the cyclotron frequency as seen in the rotating frame: one can recognize Eq. (27) as the Hamiltonian of a charged particle as seen in this frame. The cyclotron frequency is shifted by coriolis force effects. It is well-known that coriolis force caused by rotation has a form equivalent to the

Lorentz $\mathbf{v} \times \mathbf{B}$ force, so it should not be too surprising that it acts to shift the cyclotron frequency.

Note that at the Brillouin limit, where the rotation frequency is half the cyclotron frequency, Eq. (28) implies that the vortex frequency vanishes. At the Brillouin limit, particle motion as seen in the rotating frame is effectively unmagnetized.

2.5. *Total angular momentum*

Constants of the motion can be useful in understanding the dynamics of the plasma. Since the applied electromagnetic fields used to confine the plasma are (ideally) cylindrically-symmetric, the total canonical angular momentum P_θ is a conserved quantity. This quantity is a sum over the angular momentum of each particle:

$$P_\theta \equiv \sum_{i=1}^{N} (m v_{\theta i} r_i + \frac{qB}{2} r_i^2). \tag{29}$$

The first term is the usual kinetic angular momentum, and the second term is the vector-potential contribution arising from the uniform magnetic field. In a strong magnetic field, this term dominates over the first term, and one may write

$$P_\theta \approx \sum_{i=1}^{N} \frac{qB}{2} r_i^2. \tag{30}$$

In other words, the angular momentum is proportional to the mean square radius of the plasma. Since the angular momentum is a conserved quantity, the plasma mean square radius cannot change over time, which greatly limits plasma loss in a Penning trap: if any plasma charge is lost to the electrodes surrounding the plasma, other charges must compensate by moving inward so that the mean square radius is unchanged.

Note also that in a neutral plasma, with both signs of charge present, angular momentum conservation does not aid confinement in this way: a positive and a negative charge can move outward together without changing P_θ. This is what makes neutral plasmas much more difficult to confine than non-neutral plasmas.

Finally, note that in real traps, slight torques on the plasma from asymmetries in the confinement fields, or from collisions with neutral gas, cause the angular momentum to change. These torques drag on the plasma, slowing its

rotation. This makes the plasma expand radially (as well as heat) as the confining Lorentz force decreases. However, by operating in ultrahigh vacuum conditions, and by constructing the trap carefully so as to ensure a high degree of cylindrical symmetry in the electrodes, these torques can be minimized, allowing confinement times ranging from hours to even days. Also, a method known as the "rotating wall" has been used to counter-act these effects and allow infinite-time confinement. The rotating wall method will be the subject of another chapter in the series.

Question 2. Rotation of a long plasma column consisting of a single species (say, positrons) with uniform density n_0 and radius r_p, produces a magnetic field. I neglected this magnetic field in this chapter. Evaluate this self-generated magnetic field, and explain why it is a good approximation to neglect it in typical Penning trap experiments. (Hint: in typical experiments, $\omega_r r_p \ll c$.) Does the induced field enhance or reduce the applied magnetic field $B\hat{z}$?

2.6. *Solutions to the exercises*

Question 1:

(a) Square both sides of the relation $L/\lambda_D = 10$ and substitute the definition of the Debye length, Eq. (8), to obtain $L^2 e^2 n_0/(\epsilon_0 T) = 100$. Solve for n_0 using $T = 10\text{eV}$ and $L = 0.01\text{m}$, to obtain $n_0 = 5.5\times 10^{14}\text{m}^{-3}$.

(b) At the stated density and temperature, the Debye length is, according to Eq. (8), $\lambda_D = 0.743m$. This is much smaller than the size of the system, meeting criterion (9). Also, the plasma parameter as given by Eq. (11) is 4×10^7, which is much greater than unity, meeting criterion (10). At the given temperature and density, the Orion Nebula is a plasma.

Question 2: An electron column with uniform charge density $-en_0$, rotating rigidly with fluid velocity $\mathbf{u} = -\omega_r r\hat{\theta}$, will produce a current density $\mathbf{j} = en_0\omega_r r\hat{\theta}$ (where $\omega_r < 0$ for electrons). Such a current density produces a magnetic field $B_z(r)\hat{z}$. According to Ampere's law this magnetic field satisfies the differential equation $\partial B_z/\partial r = -\mu_0 j_\theta(r)$. Solving this differential equation for $B_z(r)$ using the boundary condition that outside the plasma $B_z = B$ (where B is the constant externally-applied field), yields

$$B_z(r) = -\frac{\mu_0 e n_0 \omega_r}{2}(r^2 - r_p^2) + B, r < r_p. \tag{31}$$

The total magnetic field is less than B inside the plasma (recall that for electrons $\omega_r < 0$). The maximum change from B occurs at the origin, and is given by $B - B_z(0) = -\mu_0 e n_0 \omega_r r_p^2/2$. Using Eq. (20), $\Omega_c = -eB/c$, and the identity $\mu_0\epsilon_0 =$

$1/c^2$, this expression can be rewritten as

$$B - B_z(0) = B\frac{\omega_r^2 r_p^2}{c^2}\left(1 - \frac{\omega_r}{\Omega_c}\right). \tag{32}$$

Since $|\omega_r| r_p \ll c$ in typical experiments, this expression shows that the self-generated magnetic field is negligible compared to B.

References

1. Francis Chen, *Introduction to Plasma Physics and Controlled Fusion, 2nd. Ed.*, (Springer, New York, 2006), p. 2
2. S. Ichimaru, *Basic Principles of Plasma Physics*, (W. A. Benjamin, Reading MA, 1973), p. 7
3. ibid. Ref 1, pg. 11
4. ibid. Ref 1, Sec. 3.3
5. David Pine and David Bohm, *Phys. Rev.* **92**, 609-625, (1953).
6. W. J. De Haas and P. M. Van Alphen, *Amsterdam Ac.*, **33**, 1106, (1930).
7. L. D. Landau *Z. Physik*, **64**, 629, (1930).
8. Ronald Davidson, *Theory of Nonneutral Plasmas*, (Benjamin, Reading MA, 1974)
9. Ludwig Boltzmann, *Wiener Berichte*, **76**, 373 (1887).
10. Setsuo Ichimaru, *Rev. Mod. Phys.* bf 54, 1017 (1982).
11. J. H. Malmberg and J. S. deGrassie, *Phys. Rev. Lett.* **35**, 577 (1975).
12. G. B. Andresen *et al.*, Phys. Rev. Lett. **106**, 145001 (2011).
13. B. M. Jelenkovic it et al., *Nuclear Instruments and Methods in Physics Research B* **192**, 117 (2002).
14. A. Kabantsev, *private communication.*
15. F. M. Penning,*Physica (Amsterdam)* **3**, 873 (1936).
16. D. H. E. Dubin and T. M. O'Neil, *Rev. Mod Phys.* **71**, 87 (1999).
17. J. H. Malmberg and T. M. O'Neil, *Phys. Rev. Lett.* **39** ,1333 (1977).
18. L. Brillouin, *Phys. Rev.* **67**, 260 (1945).
19. S. A. Prasad and T. M. O'Neil, *Phys. Fluids* **22**, 278 (1979).
20. P. K. Kundu, *Fluid Mechanics*, (Academic Press, San Diego, 1990)

Chapter 2

Plasma modes

This chapter explores several aspects of the linear electrostatic normal modes of oscillation for a single-species non-neutral plasma in a Penning trap. Linearized fluid equations of motion are developed , assuming the plasma is cold but collisionless, which allow derivation of the cold plasma dielectric tensor and the electrostatic wave equation. Upper hybrid and magnetized plasma waves in an infinite uniform plasma are described. The effect of the plasma surface in a bounded plasma system is considered, and the properties of surface plasma waves are characterized. The normal modes of a cylindrical plasma column are discussed, and finally, modes of spheroidal plasmas, and finite temperature effects on the modes, are briefly described.

1. Introduction. The plasma dielectric tensor.

When a single-species plasma trapped in a Penning trap is perturbed away from its equilibrium state, it rings at frequencies associated with normal modes of oscillation. These plasma modes are the subject of the following chapter. To describe the normal modes I will use a fluid theory approach as in the previous chapter, but I will further simplify by assuming the plasma is cold, neglecting the thermal pressure in the equations of motion. Also, I will describe the modes in the rotating frame of the plasma, where in equilibrium it is stationary. I will also only consider small amplitude perturbations from equilibrium, oscillating in time with frequency ω (where ω is to be determined; note that this is the frequency as seen in the *rotating frame*, Doppler-shifted with respect to the lab-frame frequency ω_{lab}).

Thus, within the plasma the density is $n(\mathbf{r},t) = n_0 + \delta n(\mathbf{r})e^{-i\omega t}$, where δn is the density perturbation, and the equilibrium density n_0 is given by Eq. (20). Also, the fluid velocity is $\mathbf{u}(\mathbf{r},t) = \mathbf{0} + \delta\mathbf{u}(\mathbf{r})e^{-i\omega t}$, and the potential is $\phi(\mathbf{r},t) = \phi_0(r,z) + \delta\phi(\mathbf{r})e^{-i\omega t}$ where ϕ_0 is the equilibrium potential (including the effective potential since we work in the rotating frame).

Then, to linear order in the perturbed quantities, the momentum equation,

Eq. (12) of the previous chapter, becomes

$$-i\omega\delta\mathbf{u} = -\frac{q}{m}\nabla\delta\phi + \Omega_v\delta\mathbf{u}\times\hat{z}. \tag{1}$$

The convective derivative $\mathbf{u}\cdot\nabla\mathbf{u}$ is dropped in Eq. (12) because it is nonlinear in $\delta\mathbf{u}$, and the vortex frequency appears rather than the cyclotron frequency because we are working in the rotating frame (see Eq. (28) of the previous chapter).

Equation(1) is linear in $\delta\mathbf{u}$ and can therefore be solved directly for $\delta\mathbf{u}$ (see Question 1). It is convenient to write this solution as

$$\delta\mathbf{u} = -\frac{\sigma\ \cdot\nabla\delta\phi}{qn_0}, \tag{2}$$

where σ is the conductivity tensor for the plasma, with components

$$\sigma = i\begin{pmatrix} \sigma_1 & i\sigma_2 & 0 \\ -i\sigma_2 & \sigma_1 & 0 \\ 0 & 0 & \sigma_3 \end{pmatrix}, \tag{3}$$

and where $\sigma_1 = \varepsilon_0\omega_p^2\omega/(\omega^2-\Omega_v^2)$, $\sigma_2 = \varepsilon_0\omega_p^2\Omega_v/(\omega^2-\Omega_v^2)$, and $\sigma_3 = \varepsilon_0\omega_p^2/\omega$. Here, I introduce the *plasma frequency* ω_p, defined in terms of the equilibrium density n_0 by

$$\omega_p \equiv \sqrt{q^2 n_0/\varepsilon_0 m}. \tag{4}$$

The plasma frequency is a natural frequency of oscillation in cold unmagnetized plasmas, as we will see.

The conductivity tensor σ expresses the linear relationship between the perturbed electric field $-\nabla\delta\phi$, and the perturbed current density $qn_0\delta\mathbf{u}$. The conductivity is a tensor rather than a scalar because an electric field in the x direction produces a current in both the x and y directions (an effect caused by the magnetic field; see Question 1).

Question 1: Prove Eqs. (2) and (3) by solving Eq. (1).

In order to obtain an equation for the mode frequencies, I will now combine Eq. (2) with the continuity equation, describing the evolution of the particle density:

$$\frac{\partial n}{\partial t} + \nabla\cdot(n\mathbf{u}) = 0. \tag{5}$$

When this equation is linearized one obtains

$$-i\omega\delta n + \nabla\cdot(n_0\delta\mathbf{u}) = 0. \tag{6}$$

Substituting for $\delta\mathbf{u}$ from Eq. (2) and solving for δn yields

$$\delta n = -\frac{i}{q\omega}\nabla\cdot(\sigma\ \cdot\nabla\delta\phi). \tag{7}$$

Finally, I combine this equation with the linearized Poisson equation, $\nabla^2\delta\phi = -\delta n/\varepsilon_0$, to obtain the following electrostatic wave equation:

$$\nabla\cdot\varepsilon\cdot\nabla\delta\phi = 0. \tag{8}$$

Here, $\varepsilon = \mathbf{1} + i\sigma/\omega\varepsilon_0$ is the frequency-dependent *plasma dielectric tensor* (where $\mathbf{1}$ is the unit tensor), with the following components:

$$\varepsilon = \begin{pmatrix} \varepsilon_1 & -i\varepsilon_2 & 0 \\ i\varepsilon_2 & \varepsilon_1 & 0 \\ 0 & 0 & \varepsilon_3 \end{pmatrix}, \tag{9}$$

and where the dielectric coefficients are

$$\begin{aligned} \varepsilon_1 &= 1 - \frac{\omega_p^2}{\omega^2 - \Omega_\nu^2}, \\ \varepsilon_2 &= \frac{\omega_p^2\Omega_\nu}{\omega(\omega^2 - \Omega_\nu^2)}, \\ \varepsilon_3 &= 1 - \frac{\omega_p^2}{\omega^2}. \end{aligned} \tag{10}$$

These coefficients follow from the components of the conductivity tensor given in Eq. (3). For example, $\epsilon_2 = \sigma_2/(\epsilon_0\omega)$. The dielectric tensor is not isotropic because the applied magnetic field and plasma rotation break the isotropy of the plasma. Note that if Ω_ν is zero, the dielectric tensor takes the unmagnetized isotropic form $\varepsilon = \varepsilon_3\mathbf{1}$.

Equation (8) contains all the information about the electrostatic cold plasma modes of oscillation. This equation shows that one can think of the plasma as a dielectric medium; the motion of charges in a normal mode polarizes the dielectric producing an electric displacement $\mathbf{D} = -\varepsilon\cdot\nabla\delta\phi$ that satisfies the Poisson equation for dielectric media, $\nabla\cdot\mathbf{D} = 0$. The problem of finding the plasma normal modes is then reduced to finding nontrivial solutions to this equation.

2. Waves in an unmagnetized plasma

Within an unmagnetized uniform single species plasma with $\Omega_\nu = 0$ (i.e. at the Brillouin limit), the dielectric is isotropic and Eq. (8) can be written as

$$\varepsilon_3\nabla^2\delta\phi = 0, \tag{11}$$

where ε_3 is given by Eq. (10). Thus, either $\nabla^2\delta\phi = 0$ which by the Poisson equation implies there is no density perturbation (and hence no mode), or $\nabla^2\delta\phi \neq 0$ and instead $\varepsilon_3 = 0$. By Eq. (10) this condition requires that $\omega = \omega_p$. This is the frequency of plasma oscillations in a cold unmagnetized uniform single-species plasma. Interestingly, the spatial form of the plasma perturbation is unimportant; all such perturbations oscillate at the plasma frequency!

To understand why the plasma rings at this frequency, consider the simple perturbation sketched in Fig. 1. A portion of the plasma in the shape of a slab is shifted slightly to the right by distance Δx. This increases the density to twice its original value in a narrow region of width Δx on the right side, and reduces it to zero in a narrow region of identical width on the left side. However, recall that there is a uniform neutralizing background that allows the unperturbed density to remain in equilibrium. Thus, the total charge density including the background in the narrow region on the right side is qn_0, and on the left side it is $-qn_0$. This configuration produces a uniform electric field E_x between the two sides:

$$E_x = -\frac{\Delta\sigma}{\varepsilon_0} = -\frac{qn_0\Delta x}{\varepsilon_0}, \tag{12}$$

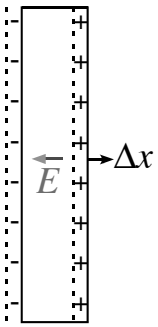

Fig. 1.: A positively-charged non-neutral plasma slab moves to the right by Δx, uncovering the neutralizing background charge on the left and overlapping the equilibrium plasma on the right

where $\Delta\sigma$ is the charge per unit area in the narrow region on the right side. This electric field acts on the slab, pulling it back toward its equilibrium posi-

tion where $\Delta x = 0$. According to Newton,

$$\Delta\ddot{x} = \frac{Q}{M} E_x = -\frac{qQn_0}{M\varepsilon_0}\Delta x, \tag{13}$$

where M and Q are the total mass and total charge of the slab respectively. However, since $Q/M = q/m$ in a single species plasma, Eq. (13) becomes $\Delta\ddot{x} = -\omega_p^2\Delta x$ (see Eq. (4)), a harmonic oscillator equation with frequency ω_p.

3. Waves in a uniform magnetized plasma

If one neglects reflections from the plasma edges, assuming that the plasma is large, one can use a Fourier representation for wave solutions in the plasma of the form

$$\delta\phi(\mathbf{r},t) = Ae^{i\mathbf{k}\cdot r - i\omega t}, \tag{14}$$

where ω and $\mathbf{k}$ are the frequency and wavenumber of a traveling wave within the plasma, and A is the wave amplitude. (Recall that for traveling waves moving in three-dimensions the wavenumber is a vector whose magnitude $k = |\mathbf{k}|$ yields the wavelength through the relation $\lambda = 2\pi/k$ and whose direction $\hat{k} = \mathbf{k}/k$ is the direction of propagation of the phase fronts of the wave.)

Waves of this form allow direct solution of Eq. (8), since $\nabla\delta\phi = i\mathbf{k}\delta\phi$. Applying Eq. (14) to Eq. (8) then yields the dispersion relation for waves in a cold uniform magnetized plasma:

$$k_\perp^2\varepsilon_1 + k_z^2\varepsilon_3 = 0, \tag{15}$$

where k_z is the component of the wave vector in the direction of the magnetic field (the z-direction) and $k_\perp$ is the magnitude of the component of the wave vector that is perpendicular to $\mathbf{B}$: $k_\perp^2 = k_x^2 + k_y^2$.

Substituting for the dielectric coefficients ε_1 and ε_3 from Eqs. (10) and rearranging terms yields a quadratic equation for ω^2. The two solutions of this quadratic correspond to two different types of propagating wave in the plasma. The frequencies of each wave can be expressed in the form

$$\omega^2 = \frac{\Omega_{uh}^2}{2} \pm \frac{\sqrt{k_\perp^2\Omega_{uh}^4 + k_z^2(\Omega_v^2 - \omega_p^2)^2}}{2k}, \tag{16}$$

where I have introduced the *upper hybrid frequency* Ω_{uh} (as seen in a rotating plasma) defined as

$$\Omega_{uh} = \sqrt{\Omega_v^2 + \omega_p^2}. \tag{17}$$

Waves with frequencies given by the upper sign in Eq. (16) are generally referred to as *upper hybrid waves*, while waves with frequencies given by the lower sign are often called *magnetized plasma waves*. The dispersion relations for each wave are plotted in Fig. 2. The frequency of each type of wave depends on the wavenumber only through its direction with respect to the magnetic field, parametrized in the figure by the ratio $k_z/k_\perp$. For waves propagating across the magnetic field, $k_z/k_\perp = 0$ and the wave frequencies for upper hybrid and magnetized plasma waves are Ω_{uh} and zero respectively. When the magnetic field vanishes, the upper hybrid waves become the unmagnetized plasma waves discussed in Sec. 2, and the magnetized plasma branch disappears. However, when the magnetic field is large so that $\Omega_v \gg \omega_p$, the dispersion relations for each branch simplify to

$$\omega^2 = \Omega_v^2 + \frac{k_\perp^2}{k^2}\omega_p^2, \quad \text{upper hybrid wave} \tag{18}$$

$$\omega^2 = \frac{k_z^2}{k^2}\omega_p^2, \qquad \text{magnetized plasma wave} \tag{19}$$

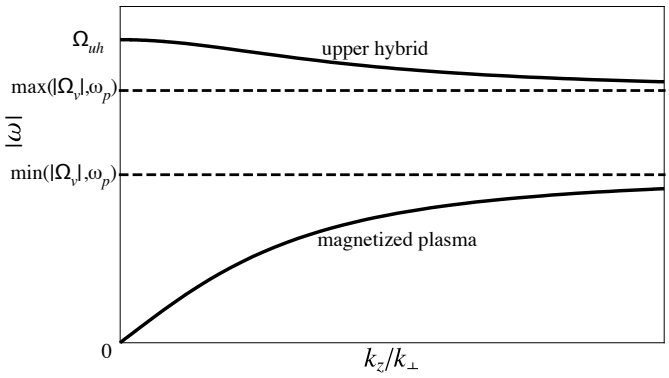

Fig. 2.: Dispersion relation for upper hybrid and magnetized plasma waves in a uniform cold plasma

In this regime upper hybrid waves can be thought of as essentially a type of cyclotron motion with a frequency that is increased by the extra restoring force associated with the plasma response (see the question below). The magnetized plasma waves are like unmagnetized plasma waves but with motion restricted to only the z direction by the strong magnetic field.

Question 2 Recall that in Sec. 2 I analyzed unmagnetized plasma oscilla-

tions by considering a slab displaced in x by Δx. Redo this calculation but keep a magnetic field pointed in the z-direction, with cyclotron frequency Ω_v.Show that the plasma now rings at frequency Ω_{uh}. (Hint: the slab moves in both the x and y directions now).

4. Modes in a Bounded Plasma

In a Penning trap, the plasma is not infinite and homogenous. This has several consequences. First, waves reflect from the plasma edges, setting up normal modes of oscillation. Most of these modes can be understood qualitatively by simply quantizing the possible values of k_z and $k_\perp$ in the previous dispersion relations obtained for homogeneous plasmas, such as Eq. (16). For instance, for a long plasma column of length L the modes have axial wave numbers that roughly satisfy $k_z = m_z\pi/L$ for integer m_z. The lowest-order axial mode, $m_z = 0$, corresponds to a potential perturbation with no z-dependence within the plasma. The next axial mode, ($m_z = 1$) has a single axial node in the center of the plasma, and so on. The possible quantized values of the perpendicular wavenumber $k_\perp$ for these modes are somewhat more difficult to categorize, requiring some algebra involving Bessel functions.

Another important finite plasma effect is the appearance of new modes associated with the plasma surface. The next subsection will analyze two types of surface plasma oscillations. For large magnetic fields they are referred to as a diocotron mode, with low frequency that scales as $1/B$, and a surface cyclotron mode, with a high frequency near the cyclotron frequency. (A third type of wave associated with the plasma surface(s), $\mathbf{E}\times\mathbf{B}$ modes, is discussed qualitatively at the end of the chapter.)

4.1. *Surface Plasma Waves*

Consider a plasma with density n_0 and a sharp edge at $x = 0$ as shown in Fig. 3. As usual there is a uniform magnetic field in the z direction. Fig. 3 could be thought of as a blow-up of a section of the plasma edge in a Penning trap plasma, with the x direction the local direction of increasing plasma radius, and the y direction in the direction of increasing θ. The plasma equilibrium is disturbed by a surface plasma wave. Such waves have potentials that are concentrated within a few wavelengths of the plasma surface. To simplify the analysis I assume that the plasma radius and the distance to surrounding conducting walls are both large relative to the wavelength of the waves.

The waves propagate along the surface of the plasma, with a perturbed po-

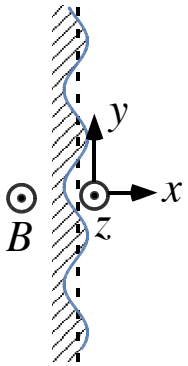

Fig. 3.: A surface plasma wave perturbs the equilibrium surface (the dotted line) at $x = 0$.

tential of the form

$$\delta\phi \propto e^{ik_y y + ik_z z - i\omega t}. \tag{20}$$

However, the x dependence of the potential is not so simple because of the plasma surface. Outside the plasma, where $x > 0$, the perturbed potential must satisfy the Laplace equation $\nabla^2 \delta\phi = 0$, which implies an exponential x dependence:

$$\delta\phi = e^{ik_y y + ik_z z - i\omega t}(Ae^{-kx} + Be^{kx}), \quad x > 0, \tag{21}$$

where A and B are undetermined constants, and $k = \sqrt{k_y^2 + k_z^2}$. Since the potential should not blow up at large x one must set $B = 0$ in Eq. (21).

On the other hand, inside the plasma these surface waves satisfy Eq. (8). Since the plasma is uniform, ε is a tensor with constant coefficients given by Eqs. (9) and (10). The equation then becomes

$$\varepsilon_1 \left(\frac{\partial^2 \delta\phi}{\partial x^2} + \frac{\partial^2 \delta\phi}{\partial y^2} \right) + \varepsilon_3 \frac{\partial^2 \delta\phi}{\partial z^2} = 0 \tag{22}$$

Substituting the assumed form for $\delta\phi$, Eq. (20), implies that

$$\varepsilon_1 \frac{\partial^2 \delta\phi}{\partial x^2} = \left(k_y^2 \varepsilon_1 + k_z^2 \varepsilon_3 \right) \delta\phi. \tag{23}$$

This differential equation has the general solution

$$\delta\phi = e^{ik_y y + ik_z z - i\omega t}(Ce^{-\kappa x} + De^{\kappa x}), \quad x < 0, \tag{24}$$

where $\kappa = \sqrt{k_y^2 + \varepsilon_3 k_z^2/\varepsilon_1}$. (For surface waves, κ is a real number, greater than zero.) The coefficient C must equal zero in order to keep the solution from blowing up at large negative values of x.

The remaining coefficients A and D are related by matching the solution across the plasma boundary at $x = 0$. Continuity of the potential implies that $A = D$. However, the laws of electromagnetism also require that the normal component of the electric displacement $\mathbf{D} = -\varepsilon \cdot \nabla\phi$ be continuous across the boundary. When applied to Eq. (24) and (21), and taking $A = D$ and $B = C = 0$, this requirement implies that

$$\hat{x} \cdot \varepsilon \cdot \nabla \; e^{\kappa x + i k_y y + i k_z z}|_{x=0} = -k\, e^{i k_y y + i k_z z}. \tag{25}$$

Applying Eq. (9) and evaluating the lhs then yields

$$\kappa\varepsilon_1 + k_y \varepsilon_2 = -k. \tag{26}$$

This is the dispersion relation for surface plasma waves. Like the dispersion relation for waves in a uniform plasma, Eq. (15), this dispersion relation depends on the direction of the wavenumber $\mathbf{k} = k_y \hat{y} + k_z \hat{z}$, but not its magnitude.

These surface waves propagate along the plasma surface, causing ripples in it's shape, but their effect on the plasma falls off exponentially with distance from the surface, with length scale κ. The motion of the plasma surface can be understood in linear wave theory as causing a surface charge (charge per unit area) $\delta\sigma(y,z,t)$. Elementary electrostatics relates the surface charge to the jump in electric field across the surface:

$$\begin{aligned} \frac{\delta\sigma}{\epsilon_0} &= \frac{\partial\delta\phi}{\partial x}|_{x=0^-} - \frac{\partial\delta\phi}{\partial x}|_{x=0^+} \\ &= A(k+\kappa)e^{i(k_y y + k_z z - \omega t)}. \end{aligned} \tag{27}$$

The surface charge is due to a small change δx in the position of the surface as shown in Fig. 3 ,

$$\delta\sigma = q n_0 \delta x. \tag{28}$$

Combining Eqs. (27) and (28) gives the change in the position of the plasma surface due to the wave:

$$\delta x = A\frac{\epsilon_0}{q n_0}(k+\kappa)e^{i(k_y y + k_z z - \omega t)}. \tag{29}$$

There are two cases where the surface wave dispersion relation can be further simplified. First, for an ummagnetized plasma with $\Omega_v = 0$, Eqs. (10) imply

that $\varepsilon_1 = \varepsilon_3 = 1 - \omega_p^2/\omega^2$ and $\varepsilon_2 = 0$, from which one may conclude that $\kappa = k$. Equation (26) then becomes

$$1 - \frac{\omega_p^2}{\omega^2} = -1$$

which has the solution $\omega^2 = \omega_p^2/2$. This gives the frequency of unmagnetized surface plasma waves. Note that the frequency is the same for any wavenumber. These unmagnetized surface plasma waves do not just appear in Penning trap plasmas at the Brillouin limit. They are also observed propagating along the surface of metals, where they are usually called *surface plasmons*.[1]

A second case that can be easily handled is when $k_z = 0$, i.e. propagation perpendicular to the magnetic field. In this case, $\kappa = k = k_y$ (assuming that k_y is positive), and Eq. (26) becomes

$$\varepsilon_1 + \varepsilon_2 = -1. \tag{30}$$

Substituting for the dielectric coefficients from Eq. (10) yields a quadratic equation for the wave frequency ω with the following two solutions:

$$\omega = -\frac{1}{2}\left(\Omega_v \pm \sqrt{\Omega_v^2 + 2\omega_p^2}\right). \tag{31}$$

Assuming that $\Omega_v > 0$, the upper sign gives the frequency of $k_z = 0$ *surface cyclotron waves*, and the lower sign yields the *diocotron wave* frequency. Although the waves have different frequencies, they both have the same value of $\kappa = k_y$ and hence the same functional form. When the vortex frequency is zero, Eq. (31) returns to the unmagnetized surface plasma frequencies, but when $|\Omega_v| >> \omega_p$, the two surface waves have the following approximate frequencies:

$$\omega \approx -\Omega_v - \frac{\omega_p^2}{2\Omega_v}, \text{ surface cyclotron wave} \tag{32}$$

$$\omega \approx \frac{\omega_p^2}{2\Omega_v}, \qquad \text{diocotron wave} \tag{33}$$

The frequency of the diocotron wave in this large magnetic field regime scales as $1/B$ since in this regime $\Omega_v \sim \Omega_c = qB/m$. Also, in this regime the diocotron wave frequency (as seen in the frame rotating with the plasma) is the same as the plasma rotation rate itself (see Eq. (21) in the previous chapter).

The sign of the frequency for these two surface waves has physical significance. Assuming $k_z = 0$, $k_y > 0$, and a positively-charged plasma, the surface cyclotron wave described by Eq. (32) has negative frequency and a phase velocity in the $-y$ direction, while diocotron wave travels in the opposite $+y$ direction (as seen in the rotating frame where the equilibrium plasma is stationary).

On a cylindrical plasma the $-y$ direction corresponds to the -θ direction, so the surface cyclotron wave rotates around the plasma column in the same direction as the cyclotron motion of single particles. This is as opposed to the upper hybrid waves, which are in a similar frequency regime but can rotate in either direction on the plasma column.

Question 3 Show that in general there are two solutions to Eq. (26) for the surface wave frequency *provided that* $\omega_p/|\Omega_v| \geq |k_z|/k$.

Question 4 Show that these solutions are

$$\omega = \frac{-k_y\Omega_v \pm \sqrt{2k^2\omega_p^2 + \Omega_v^2(k_y^2+2k_z^2)}}{2k}. \tag{34}$$

Question 5 Show that the values of κ for the two solutions are identical, for given values of the other parameters.

The dispersion curves given by Eq. (34) are plotted in Fig. 4 versus the direction of propagation of the waves as parametrized by k_z/k, and for three different magnetic field strengths, assuming $k_y \geq 0$ and a positively-charged plasma. In Fig. 5 the value of κ/k is plotted. Note that in the large magnetic field limit, only $k_z = 0$ surface waves are allowed, but when $|\Omega_v|/\omega_p \leq 1$ waves may propagate along the surface in any direction. As $|\Omega_v|/\omega_p$ increases, the surface cyclotron frequency also increases in magnitude, following the (negative of) the cyclotron frequency, while the behavior of the diocotron branch is a bit more complicated: for small k_z/k the frequency decreases with increasing $|\Omega_v|$, as expected from Eq. (31) or Eq. (33), while for larger k_z/k the frequency can increase with increasing $|\Omega_v|$. For propagation parallel to **B** (which requires $|\Omega_v|/\omega_p < 1$), the two surface waves have equal but opposite frequencies, $\omega = \pm\Omega_{uh}/\sqrt{2}$. In this case one might refer to the waves as surface upper hybrid waves.

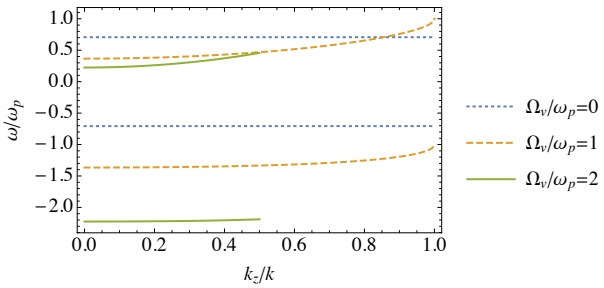

Fig. 4.: Dispersion curves for the two surface plasma waves versus propagation direction, for three different magnetic field strengths.

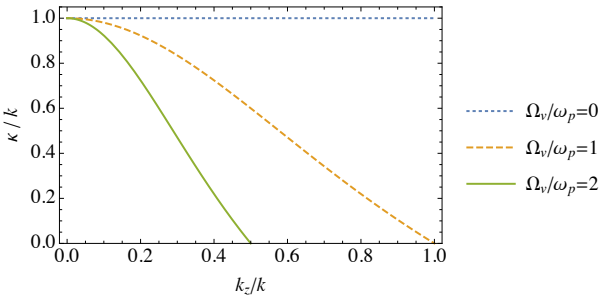

Fig. 5.: Inverse decay length κ for surface plasma waves versus propagation direction, for three different magnetic field strengths.

4.2. *Cylindrical Plasmas*

Plasma modes can be determined analytically in several other geometries of importance to Penning trap experiments. For a long uniform density plasma column of radius r_p and length L, running from $z = 0$ to $z = L$, and trapped along the axis of a hollow conducting cylinder of radius r_w, the dispersion relation involves Bessel function solutions of Eq. (8), and is called the Trivelpiece-Gould (TG) dispersion relation.[2] The following remarks assume the reader's familiarity with basic properties of Bessel functions.

Within the plasma, where the tensor ϵ is uniform in space, Eq. (8) can be expressed in cylindrical coordinates (r,θ,z) as

$$\varepsilon_1\left(\frac{1}{r}\frac{\partial}{\partial r}r\frac{\partial\delta\phi}{\partial r}+\frac{1}{r^2}\frac{\partial^2\delta\phi}{\partial\theta^2}\right)+\varepsilon_3\frac{\partial^2\delta\phi}{\partial z^2}=0. \tag{35}$$

This differential equation is separable and the solution that is finite at the origin is

$$\delta\phi(\mathbf{r},t)=AJ_{m_\theta}(k_\perp r)\cos(k_z z)e^{im_\theta\theta-i\omega t},\quad r<r_p, \tag{36}$$

where the non-negative integer m_θ is the azimuthal mode number, $k_z = m_z\pi/L$ where m_z is also a nonnegative integer, and J_{m_θ} is a Bessel function of the first kind.[19] The transverse wavenumber $k_\perp$ is a separation constant that depends on k_z and ω through Eq. (15):

$$k_\perp^2=-k_z^2\epsilon_3/\epsilon_1. \tag{37}$$

The cosine form of the z dependence is chosen so that the axial electric field vanishes at the ends of the plasma column. For finite length plasma columns this is a useful but rough approximation that improves as the length of the column increases.[18,20]

Outside the plasma, the potential satisfies Laplace's equation (i.e. $\epsilon_1 = \epsilon_3 = 1$ in Eq. (35)), and also vanishes at the conducting cylinder. The solution in this region is

$$\delta\phi(\mathbf{r},t) = B\left(I_{m_\theta}(k_z r)K_{m_\theta}(k_z r_w) - I_{m_\theta}(k_z r_w)K_{m_\theta}(k_z r)\right) \times \cos(k_z z)e^{im_\theta\theta - i\omega t}, \quad r > r_p, \tag{38}$$

where I_{m_θ} and K_{m_θ} are Bessel functions of the second kind.[19] The coefficient B and the mode frequency ω are determined by matching the interior solution, Eq. (36), to the above exterior solution. The potential must be continuous, implying that

$$AJ_{m_\theta}(k_\perp r_p) = B\left(I_{m_\theta}(k_z r_p)K_{m_\theta}(k_z r_w) - I_{m_\theta}(k_z r_w)K_{m_\theta}(k_z r_p)\right). \tag{39}$$

Also, integration of Eq. (8) from $r = r_p^-$ to $r = r_p^+$ implies that

$$\hat{r}\cdot\epsilon\cdot\nabla\delta\phi|_{r_p^-} = \frac{\partial\delta\phi}{\partial r}|_{r_p^+}. \tag{40}$$

This result merely expresses the continuity of the normal component of the electric displacement $\mathbf{D} = \epsilon\cdot\nabla\delta\phi$ across the plasma surface, as discussed previously (see Eq. (25)). Substituting for $\delta\phi$ from Eqs. (36) and (38) and using Eq. (10) yields

$$A\epsilon_1\frac{\partial}{\partial r_p}J_{m_\theta}(k_\perp r_p) + A\epsilon_2\frac{m_\theta}{r_p}J_{m_\theta}(k_\perp r_p) = B\frac{\partial}{\partial r_p}\left(I_{m_\theta}(k_z r_p)K_{m_\theta}(k_z r_w) - I_{m_\theta}(k_z r_w)K_{m_\theta}(k_z r_p)\right). \tag{41}$$

Substituting for A from Eq. (39) yields the relation

$$\epsilon_1\frac{\partial}{\partial r_p}J_{m_\theta}(k_\perp r_p) + \epsilon_2\frac{m_\theta}{r_p}J_{m_\theta}(k_\perp r_p) = J_{m_\theta}(k_\perp r_p)\frac{\frac{\partial}{\partial r_p}\left(I_{m_\theta}(k_z r_p)K_{m_\theta}(k_z r_w) - I_{m_\theta}(k_z r_w)K_{m_\theta}(k_z r_p)\right)}{I_{m_\theta}(k_z r_p)K_{m_\theta}(k_z r_w) - I_{m_\theta}(k_z r_w)K_{m_\theta}(k_z r_p)}. \tag{42}$$

Equation (42) together with Eq. (37) is the Trivelpiece-Gould dispersion relation. In general it yields real solutions for the mode frequency ω, but the solutions must be determined numerically. However, there are several limits where the dispersion relation can be simplified. For instance, when $k_z r_w \ll 1$ the rhs

simplifies to yield

$$\epsilon_1 r_p \frac{\partial}{\partial r_p} J_{m_\theta}(k_\perp r_p) + \epsilon_2 m_\theta J_{m_\theta}(k_\perp r_p)$$
$$= J_{m_\theta}(k_\perp r_p) \begin{cases} -m_\theta \frac{1+(r_p/r_w)^{2m_\theta}}{1-(r_p/r_w)^{2m_\theta}}, & m_\theta > 0, \\ -\frac{1}{\ln(r_w/r_p)}, & m_\theta = 0. \end{cases} \quad (43)$$

Several other simplifications can be made in various regimes, as described below.

The TG dispersion relation provides mode frequencies as seen in a frame rotating with the plasma. In the lab frame, there is a Doppler-shift of the frequency caused by this rotation. The lab coordinate θ_{lab} is related to the rotating framing coordinate θ by a Galilean transformation, $\theta_{lab} = \theta - \omega_r t$. The factor $\exp[i m_\theta \theta - i\omega t]$ in the mode potential can then be written in lab frame coordinates as $\exp[i m_\theta \theta_{lab} - i(\omega - m_\theta \omega_r)t]$. This implies that the lab frame frequency is

$$\omega_{lab} = \omega - m_\theta \omega_r. \quad (44)$$

Figure 6 displays a sketch of the TG mode frequencies for a given value of $k_z \neq 0$ and $m_\theta \neq 0$, versus magnetic field. Also shown, as dashed lines, are the upper hybrid frequency and the vortex frequency. The plot for $m_\theta = 0$ has the appearance of the upper half of Fig. 6 reflected about the x-axis into the lower half (i.e. the $m_\theta = 0$ modes come in $\pm\omega$ pairs).

The modes fall into three classes: upper hybrid modes, magnetized plasma modes, and two surface modes. The upper hybrid modes have frequencies in the range $\max(\omega_p^2, \Omega_v^2) < \omega^2 < \Omega_{uh}^2$. The magnetized plasma modes are in the range $\omega^2 < \min(\omega_p^2, \Omega_v^2)$. These ranges are the same as for a plasma with no boundaries; see Fig. 2.These modes have an infinite number of possible branches with different values of $k_\perp$ for each, corresponding to different numbers of radial oscillations within the plasma column.

As Ω_v becomes large, and provided that $k_z \neq 0$, the positive frequency surface mode converts to a magnetized plasma mode with no radial nodes. For $k_z \neq 0$ and $m_\theta > 0$ the negative frequency surface mode joins the upper hybrid modes for large Ω_v; and for $m_\theta = 0$ this mode instead joins the magnetized plasma modes.

In the $k_z = 0$ limit, discussed below, the two surface modes remain separate for all Ω_v; they are the diocotron and surface cyclotron modes. In this limit all the upper hybrid branches are degenerate with $\omega = \pm\Omega_{uh}$ and the magnetized plasma modes all have $\omega = 0$, just as for an unbounded plasma (see Fig. 2).

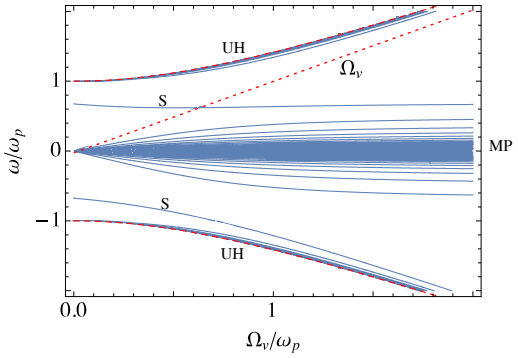

Fig. 6.: A sketch of the frequencies of TG modes on a cylindrical plasma column versus the vortex frequency Ω_v for fixed values of $k_z > 0$ and $m_\theta > 0$. Dashed lines show the positive and negative upper hybrid frequencies and the vortex frequency. Modes labeled S, UH, and MP are surface modes, upper hybrid modes, and magnetized plasma modes respectively. The infinite set of upper hybrid modes are too close together to be distinguished in this sketch.

4.2.1. *Trivelpiece-Gould magnetized plasma modes*

The TG plasma modes are finite k_z magnetized plasma oscillations on the cylindrical column, with a frequency of order the plasma frequency or less. For simplicity, I will consider the dispersion relation for these modes assuming that $k_z r_w \ll 1$ and taking the strong magnetic field limit where $\omega_p \ll \Omega_v$. One can then approximate $\epsilon_1 = 1$. The mode frequency then follows from Eq. (37):

$$\omega^2 = \frac{\omega_p^2 k_z^2}{k_\perp^2 + k_z^2}, \tag{45}$$

This is the same as Eq. (19) for a plasma with no boundaries. These TG modes are magnetized cold plasma waves with k_z and $k_\perp$ quantized by the finite plasma length and radius. The possible values of $k_\perp$ follow from Eq. (43), taking

$\epsilon_1 = 1$ and $\epsilon_2 = 0$ (the latter assumes that $k_z/k_\perp \gg \omega_p/|\Omega_v|$):

$$r_p \frac{\partial}{\partial r_p} J_{m_\theta}(k_\perp r_p) = J_{m_\theta}(k_\perp r_p) \begin{cases} -m_\theta \frac{1+(r_p/r_w)^{2m_\theta}}{1-(r_p/r_w)^{2m_\theta}}, & m_\theta > 0, \\ -\frac{1}{\ln(r_w/r_p)}, & m_\theta = 0. \end{cases} \tag{46}$$

There are multiple solutions to Eq. (46) corresponding to waves with different numbers of radial nodes within the plasma column. For example, for $m_\theta = 0$ there is a solution with no radial nodes that roughly satisfies

$$k_\perp r_p = \sqrt{\frac{2}{\ln(r_w/r_p)}}, \tag{47}$$

assuming that $r_w \gg r_p$. (This follows by Taylor expansion of the $m_\theta = 0$ Bessel functions in Eq. (46) around $k_\perp r_p = 0$, assuming that $k_\perp r_p \ll 1$.) The solutions with more nodes roughly satisfy $J_1(k_\perp r_p) = 0$, so that

$$k_\perp = j_{1,n}/r_p, \quad n = 1,2,3,... \tag{48}$$

where $j_{m_\theta,n}$ is the n'th zero of the Bessel function $J_{m_\theta,n}(x)$, counting out from, but not including, the origin.

For $m_\theta > 0$, and again assuming $r_w \gg r_p$, the rhs of Eq. (46) can be approximated as $-m_\theta J_{m_\theta}$. Then a Bessel function identity[19] allows one to write the equation as $k_p r_p J_{m_\theta - 1}(k_\perp r_p) = 0$, so that the solutions for $k_\perp$ are

$$k_\perp = j_{m_\theta - 1,n}/r_p, \quad n = 1,2,3,.... \tag{49}$$

These solutions correspond to a potential with $n-1$ radial nodes. The $n = 1$ case with no radial nodes and with positive frequency (for $\Omega_v > 0$) connects to the positive frequency surface mode; see Fig. 6.

The formulae in this section, while useful in their regimes of validity, are only approximate. The frequencies found by solving the full TG dispersion relation can differ from these formulae, sometimes substantially, depending on the circumstances. Two examples are shown in Fig. 7. The solid curves are frequencies versus wavenumber k_z, obtained from the full dispersion relation for a plasma with $r_w/r_p = 4, \Omega_v/\omega_p = 10$, and $m_\theta = 0$ in (a) and $m_\theta = 2$ in (b). The dotted curve in (a) is Eq. (47), and the dashed curves are Eq. (48), both combined with Eq. (45). In Fig.7(b) the dashed curves are Eqs. (49) and (45). The approximate dispersion relations are just that, approximate, particularly for small $k_z r_p$ in the $m_\theta = 2$ example, where the assumption that $k_z/k_\perp \gg \omega_p/\Omega_v$ is breaking down and the ϵ_2 term in the TG dispersion relation cannot be neglected. Here the upper TG mode is becoming a surface mode, poorly described by Eq. (45), and the other modes are not well-described by Eq. (49). [In fact, one

can show[18] that for $k_z/k_\perp < \omega_p/\Omega_v$ and $m_\theta \neq 0$ the TG modes (other than the surface mode) are better-described by $k_\perp = j_{m_\theta,n}/r_p$ rather than Eq. (49).]

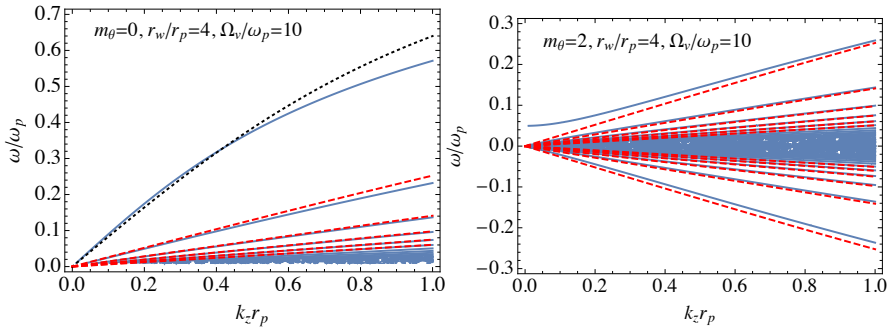

Fig. 7.: Frequency versus wavenumber for TG modes with $|\omega| < \omega_p$. Solid curves are solutions of the full TG dispersion relation, Eq. (42). Dotted and dashed curves are approximate analytic dispersion relations described in the text. Only the first six approximate dispersion curves are shown, corresponding to waves with between zero and five radial nodes.

4.2.2. *Upper hybrid modes*

In the large magnetic field regime $|\Omega_v| \gg \omega_p$ there is also a set of upper hybrid modes whose frequencies have a magnitude close to that of the cyclotron frequency $|\Omega_v|$. For these modes one can set $\epsilon_3 = 1$, which implies through Eq. (37) that $\epsilon_1 = -k_z^2/k_\perp^2$. Using Eq. (10) this equation can be rewritten as

$$\omega^2 = \Omega_v^2 + \frac{k_\perp^2}{k_\perp^2 + k_z^2}\omega_p^2, \tag{50}$$

the upper hybrid dispersion relation in the strong magnetic field regime. This dispersion relation is the same as Eq. (18), except that now k_z and $k_\perp$ are quantized. The possible values of $k_\perp$ follow from Eq. (42), or (43) if $k_z r_w \ll 1$ (I will assume this here for simplicity). In the large magnetic field regime with $\omega \sim \pm\Omega_v$, one may set $\epsilon_1 = -k_z^2/k_\perp^2$ and $\epsilon_2 = \pm(1-\epsilon_1) = \pm(1+k_z^2/k_\perp^2)$, so that Eq. (43)

becomes

$$-k_z^2 r_p \frac{\partial}{\partial r_p} J_{m_\theta}(k_\perp r_p) \pm (k_\perp^2 + k_z^2) m_\theta J_{m_\theta}(k_\perp r_p)$$
$$= k_\perp^2 J_{m_\theta}(k_\perp r_p) \begin{cases} -m_\theta \frac{1+(r_p/r_w)^{2m_\theta}}{1-(r_p/r_w)^{2m_\theta}}, & m_\theta > 0, \\ -\frac{1}{\ln(r_w/r_p)}, & m_\theta = 0, \end{cases} \tag{51}$$

where the $\pm$ sign in the equation corresponds to $\omega \sim \pm\Omega_v$. Upper hybrid modes with positive ω and m_θ have a positive azimuthal phase velocity, and generally do not have the same $k_\perp$ as modes which rotate on the column in the negative azimuthal direction because the magnetic field breaks the reflection symmetry normally associated with these two directions.

There are multiple solutions to Eq. (51) for $k_\perp$, corresponding to upper hybrid modes with different numbers of radial nodes. One simple case is $k_z = 0$ (i.e $m_z = 0$), where the solutions are $k_\perp = j_{m_\theta,n}/r_p$, $n = 1,2,3,....$ These solutions correspond to a z-independent potential that vanishes outside the plasma. These upper hybrid modes are internal waves with n radial nodes (not counting the node at $r = 0$ for $m_\theta \neq 0$), one of which is at the plasma edge. These modes have no effect outside the plasma, and hence cannot be observed or excited using external electrodes. All of these waves have the same frequency (as seen in the rotating frame), the upper hybrid frequency $\pm\Omega_{uh}$.

Another simple case is $\omega < 0$, $m_\theta > 0$, and $(r_p/r_w)^{2m_\theta} \ll 1$, so that the rhs in Eq. (51) can be approximated as $-m_\theta k_\perp^2 J_{m_\theta}$. Then for the lower sign in the equation corresponding to $\omega < 0$, a Bessel function identity[19] allows one to rewrite Eq. (51) as $-k_z^2 k_\perp r_p J_{m_\theta - 1}(k_\perp r_p) = 0$. Thus, in this case the solutions for $k_\perp$ are

$$k_\perp = j_{m_\theta - 1,n}/r_p, \ , n = 1,2,3,.... \tag{52}$$

These solutions have a potential with $n-1$ radial nodes within the plasma column (again, not counting the node at $r = 0$). The $n = 1$ case has no radial nodes and connects to a surface mode; see Fig. 6.

In using these formulae, remember that the same caveat with respect to their approximate nature holds as for the magnetized plasma modes discussed in the previous section.

4.2.3. *Surface modes for an unmagnetized cylindrical plasma*

At the Brillouin limit where $\Omega_v = 0$, the plasma is unmagnetized when seen in the rotating frame, and the TG mode dispersion relation simplifies. In this

limit $\epsilon_2 = 0$ and $\epsilon_1 = \epsilon_3$ so Eq. (37) implies $k_\perp^2 = -k_z^2$; i.e. $k_\perp$ is imaginary. In this case the Bessel functions of the first kind convert to Bessel functions of the second kind through the identity $J_{m_\theta}(ix) = i^{m_\theta} I_{m_\theta}(x)$. These Bessel functions of the second kind are exponentially large for large argument, implying that the modes are surface modes concentrated at $r = r_p$. The frequency of these modes follows from Eq. (42):

$$\epsilon_3 = 1 - \omega_p^2/\omega^2 = \\ = \frac{I_{m_\theta}(k_z r_p)}{\frac{\partial}{\partial r_p} I_{m_\theta}(k_z r_p)} \frac{\frac{\partial}{\partial r_p}\left(I_{m_\theta}(k_z r_p)K_{m_\theta}(k_z r_w) - I_{m_\theta}(k_z r_w)K_{m_\theta}(k_z r_p)\right)}{I_{m_\theta}(k_z r_p)K_{m_\theta}(k_z r_w) - I_{m_\theta}(k_z r_w)K_{m_\theta}(k_z r_p)}. \quad (53)$$

which can be easily solved for ω^2. In the limit of large m_θ or large k_z, the rhs simplifies to -1, yielding $\omega^2 = \omega_p^2/2$, giving the surface plasma frequency familiar from the slab geometry case considered previously.

As the magnetic field increases from zero, eventually ϵ_1/ϵ_3 changes sign, $k_\perp$ becomes real, and (for $k_z \neq 0$) the two surface modes join the magnetized plasma and (for $m_\theta \neq 0$) upper hybrid branches, as discussed in relation to Fig. 6.

4.2.4. *Diocotron modes and surface cyclotron modes*

Another simplifying limit of the TG dispersion relation is when $k_z \to 0$ and $m_\theta \neq 0$. In this limit Eq. (37) implies $k_\perp \to 0$ as well, provided that $\epsilon_1 \neq 0$ so that we avoid the upper hybrid modes discussed previously. Taylor expansion of Eq. (43) in $k_\perp$ then yields

$$m_\theta(\epsilon_1 + \epsilon_2) = -m_\theta \frac{1 + (r_p/r_w)^{2m_\theta}}{1 - (r_p/r_w)^{2m_\theta}}. \quad (54)$$

This is the dispersion relation for $k_z = 0$ surface waves on the cylindrical plasma column. Comparing to Eq. (30), Eq. (54) differs from the previous slab-geometry result only through the terms involving $(r_p/r_w)^{2m_\theta}$. These terms encode the effect on the mode of image charges in the cylindrical electrodes, which were neglected in the slab-geometry discussion of surface waves. The slab geometry result is approached when m_θ is large or when $r_p/r_w \to 0$, so that $(r_p/r_w)^{2m_\theta} \to 0$, i.e. when image charge effects are negligible.

Equation (54) can be solved for ω to yield two roots:

$$\omega = -\frac{\Omega_v}{2} \pm \sqrt{\frac{\Omega_v^2}{4} + \omega_p^2 \frac{1 - (r_p/r_w)^{2m_\theta}}{2}}. \quad (55)$$

When $\Omega_v = 0$ the roots are equal and opposite and correspond to the surface plasma waves discussed in the previous section, shifted in frequency by image charge effects. For large Ω_v these roots correspond to a high frequency surface cyclotron mode and a low frequency diocotron mode. For $\Omega_v^2 \gg \omega_p^2$ the low frequency solution is

$$\omega = \frac{\omega_p^2}{2\Omega_v}\left[1-\left(\frac{r_p}{r_w}\right)^{2m_\theta}\right], \tag{56}$$

the *diocotron frequency* (as seen in the rotating frame). The surface cyclotron frequency (as seen in the rotating frame) is given by $\Omega_v - \omega$, where ω is the diocotron frequency. Equation (56) is identical to the slab geometry diocotron wave frequency in the large magnetic field limit, Eq. (33), except for a frequency shift caused by the effect of image charges in the conducting wall.

The functional form of the diocotron and surface cyclotron mode potential inside and outside the plasma is given by Eq. (36) and (38), taking $k_\perp \to 0$ and using Taylor expansions for the Bessel functions:

$$\delta\phi(\mathbf{r},t) = Ce^{i(m_\theta\theta-\omega t)}\begin{cases} r^{m_\theta}, & r<r_p, \\ \frac{r^{m_\theta}-(r_w^2/r)^{m_\theta}}{1-(r_w/r_p)^{2m_\theta}}, & r>r_p. \end{cases} \tag{57}$$

This potential corresponds to a z-independent distortion of the shape of the plasma, producing a travelling wave on the plasma surface that propagates in the θ direction. The radial change $\delta r(\theta,t)$ in the position of the plasma surface due to the mode can be obtained using an argument similar to that which led to Eq. (29), and is left as an exercise (see below). For instance, the $m_\theta = 1$ mode is a displacement of the entire column off of the axis of symmetry of the conducting cylinder. The off-axis plasma is attracted to its image in the conducting walls and this force, for the diocotron mode, causes the entire plasma to $\mathbf{E}\times\mathbf{B}$ drift around the cylinder. The $m_\theta = 1$ surface cyclotron mode has the same distortion, except that its motion is at higher frequency: it is essentially cyclotron motion of the entire column, with a frequency slightly shifted by image charge forces. Both modes rotate in the same direction as seen in the lab frame: the direction of the cyclotron motion (i.e. the negative $\hat{\theta}$ direction for positive charges).

Question 6 Using Eq. (57) show that the radial change δr in the position of the plasma surface produced in a surface cyclotron or diocotron mode is given by

$$\delta r = C\frac{2\epsilon_0 m_\theta r_p^{m_\theta-1}}{qn_0\left[1-(r_p/r_w)^{2m_\theta}\right]}e^{i(m_\theta\theta-\omega t)}. \tag{58}$$

4.3. *Other geometries;* $\mathbf{E}\times\mathbf{B}$ *modes; finite temperature effects*

Plasma modes can be determined analytically in a few other geometries of importance to Penning trap experiments. For instance, for spheroidal plasmas of small size compared to the distance to the electrodes, the dispersion relation has been worked out in terms of Legendre functions.[3,9] The functional form of this dispersion relation will not be discussed further here; the interested reader is referred to the references.

The modes of a spheroid consist of upper hybrid waves, magnetized plasma waves, and surface waves, each with quantized wave numbers, just as for the TG dispersion relation. However, in the strong magnetic field regime there is also an extra set of modes: modes with low frequencies of order $1/B$, that consist of vortical $\mathbf{E}\times\mathbf{B}$ motions in the $x-y$ plane.[4] These modes differ from the diocotron surface mode (which also has frequency of order $1/B$) in that they have finite frequency due only to the varying axial length of the spheroid as a function of cylindrical radius. As an axial rod of plasma is convected radially by $\mathbf{E}\times\mathbf{B}$ motion, it feels a restoring force due to the different length of the plasma at that radius, which compresses (or expands) the rod.[5] In a cylindrical plasma column with flat ends, such motions would merely rearrange the fluid elements within the column without changing the density or potential; there would be no linear restoring force and the motions would be inherently nonlinear. These "zero-frequency" nonlinear motions are referred to as *convective cells*, and are important in the study of plasma turbulence.[6] Variation of the equilibrium length of the plasma column with radius breaks the degeneracy of the convective cells, giving them a range of low but finite frequencies.

An analogy has also been drawn between these $\mathbf{E}\times\mathbf{B}$ modes and certain low-frequency oceanic and atmospheric disturbances called *Rossby waves*.[7] Radial variation of the plasma length can be thought of as analogous to the longitudinal variation in coriolis force that drives these waves in the ocean and the atmosphere.[8] This analogy could allow simulation of geophysical phenomena in a non-neutral plasma.

Within the plasma spheroid these finite-length $\mathbf{E}\times\mathbf{B}$ modes are nearly z-independent, and as $|\Omega_v|/\omega_p$ is reduced below unity they convert to magnetized plasma modes with small axial wave numbers and hence low frequencies, approaching zero frequency as $\Omega_v \to 0$ (see Fig. 2).

For simplicity, the theory of plasma waves considered in this chapter neglected effects associated with finite temperature. Finite temperature effects on magnetized plasma modes[10,11] and diocotron modes[12] have been observed and studied theoretically; rather less is known concerning these effects on sur-

face cyclotron and upper hybrid modes although work is ongoing.[13,14] For example, the magnetized plasma mode frequencies are shifted upward by finite temperature as plasma pressure increases the wave restoring force. These shifts are sufficiently well-understood to be used as a plasma thermometer in some experiments.[15–17]

Furthermore, finite temperature effects can produce mode damping through the process called *Landau damping*,[21] in which charged particles moving with nearly the same velocity as the wave phase velocity (due to the particle's thermal speed) are resonantly accelerated by the wave potential and hence remove energy from the wave.

In addition, a new set of temperature-dependent modes with frequencies near multiples of the cyclotron frequency are predicted to occur at finite temperature.[13,22] These "Bernstein modes" have been observed in recent experiments on non-neutral plasmas,[14,22] but more work is needed to fully understand their dispersion and damping in such plasmas.

4.4. *Solutions to the exercises*

Question 1

Equation (1) has three components,

$$\begin{aligned}
-i\omega\delta u_x &= -\frac{q}{m}\frac{\partial\delta\phi}{\partial x} + \Omega_v \delta u_y, \\
-i\omega\delta u_y &= -\frac{q}{m}\frac{\partial\delta\phi}{\partial y} - \Omega_v \delta u_x, \\
-i\omega\delta u_z &= -\frac{q}{m}\frac{\partial\delta\phi}{\partial z}.
\end{aligned}$$

The last equation implies $\delta u_z = -iq/(m\omega)\partial\delta\phi/\partial z$. The first two equations are coupled, but can be easily solved to yield

$$\begin{aligned}
\delta u_x &= -\frac{iq}{m}\frac{\omega\partial\delta\phi/\partial x + i\Omega_v\partial\delta\phi/\partial y}{\omega^2-\Omega_v^2}, \\
\delta u_y &= -\frac{iq}{m}\frac{\omega\partial\delta\phi/\partial y - i\Omega_v\partial\delta\phi/\partial x}{\omega^2-\Omega_v^2}.
\end{aligned}$$

This solution can be written in matrix form as shown in Eqs. (2) and (3).

Question 2

Referring to Fig. 1, there is now a magnetic field out of the page (in the z direction). The magnetic field modifies the equations of motion of the plasma

slab, so that Eq. (13) is replaced by the coupled equations

$$\Delta\ddot{x} = -\omega_p^2 \Delta x + \Delta\dot{y}\Omega_v,$$
$$\Delta\ddot{y} = -\Delta\dot{x}\Omega_v.$$

Integrating the second equation to obtain $\Delta\dot{y} = -\Delta x\Omega_v$, and substituting this into the first equation, yields $\Delta\ddot{x} = -(\omega_p^2 + \Omega_v^2)\Delta x$. This harmonic oscillator equation implies that position of the slab oscillates at the upper hybrid frequency.

Questions 3,4

Write Eq. (26) as $\kappa\epsilon_1 = -k - k_y\epsilon_2$, square both sides, and substitute $\kappa^2 = k_y^2 + \epsilon_3 k_z^2/\epsilon_1$. This yields $k^2 + 2k k_y\epsilon_2 + k_y^2\epsilon_2^2 = k_y^2\epsilon_1^2 + k_z^2\epsilon_3\epsilon_1$. Using the definitions of ϵ_1, ϵ_2, and ϵ_3, this equation can be expressed as

$$\frac{2k^2\omega^2 + 2k k_y\omega\Omega_v - k^2\omega_p^2 - k_z^2\Omega_v^2}{\omega^2\left(\omega^2 - \Omega_v^2\right)} = 0.$$

The numerator is a quadratic function of ω, whose solution is given by Eq. (34). However, this solution arises from squaring both sides of the original equation, so there is an extra requirement : $\kappa\epsilon_1$ must have the same sign as $-k - k_y\epsilon_2$. Assuming that κ is real (see the solution to Question 5), the sign of ϵ_1 must be the same as $-k - k_y\epsilon_2$. We have already shown this to be the case at $k_z = 0$, where $\epsilon_1 = -1 - \epsilon_2$ (and $k = k_y$), so as k_z/k increases from zero the sign changes only where $-k - k_y\epsilon_2$ passes through zero. This expression can be written as

$$\frac{k\omega\Omega_v^2 - k\omega^3 - k_y\Omega_v\omega_p^2}{\omega(\omega^2 - \Omega_v^2)}.$$

However, using Eq. (34) this becomes

$$\frac{k^2\omega_p^2 - k_z^2\Omega_v^2}{2k(\omega^2 - \Omega_v^2)},$$

which changes sign when $k_z^2/k^2 = \omega_p^2/\Omega_v^2$.

Question 5

Substitute Eq. (34) into $\kappa^2 = k_y^2 + \epsilon_3 k_z^2/\epsilon_1$. After some algebra, one obtains the expression

$$\kappa^2 = k^2\left(\frac{k^2\omega_p^2 - k_z^2\Omega_v^2}{k^2\omega_p^2 + k_z^2\Omega_v^2}\right)^2, \tag{59}$$

independent of the sign of the square root in Eq. (34). This expression also shows that κ is real.

Question 6

The change in radial position δr of the plasma surface is related to a surface charge $\delta\sigma$ through $\delta r = \delta\sigma/(qn_0)$. The surface charge is related to the jump in radial electric field across the surface (see Eq. (27)): $\delta\sigma/\epsilon_0 = \frac{\partial\delta\phi}{\partial r}|_{r=r_p^-} - \frac{\partial\delta\phi}{\partial r}|_{r=r_p^+}$. Substituting for $\delta\phi$ from Eq. (57) leads directly to Eq. (58).

References

1. R. H. Ritchie, *Physical Review* **106**, 874 (1957).
2. A. W. Trivelpiece and R. W. Gould, *Jour. Appl. Phys.* **30** 1784 (1959).
3. D. H. E. Dubin, *Phys. Rev. Lett.* **66**, 2076 (1991).
4. D. H. E. Dubin, *Phys. Rev. E* **53**, 5268 (1996).
5. T. J. Hilsabeck and T. M. O'Neil, *Phys. Plasmas* **8**, 407 (2001).
6. J. A. Krommes, *Statistical Descriptions and Plasma Physics*, Chapter 5.5 in *Handbook of Plasma Physics, vol. II*, edited by M. Rosenbluth and R. Sagdeev (North-Holland, Amsterdam, 1984), p. 183.
7. C. G. Rossby, *J. Marine Research* **2**, 38 (1939).
8. J. M. Finn, D. del Castillo-Negrete, and D. C. Barnes, *Phys. Plasmas* **6**, 3744 (1999).
9. J. J. Bollinger *et al.*, *Phys. Rev. A* **48**, 525 (1993).
10. F. Anderegg *et al.*, *Phys. Rev. Lett.* **90**, 115001 (2003).
11. M. D. Tinkle *et al.*, *Phys. Rev. Lett.* **72**, 354 (1994).
12. K. S. Fine and C. F. Driscoll, *Phys. Plasmas* **5**, 601 (1998).
13. D. H. E. Dubin, *Phys. Plasmas* **20** 042120, (2013).
14. M. Affolter, F. Anderreg, D. H. E. Dubin and C. F. Driscoll, *Phys. Lett. A* **378**, 2406 (2014).
15. M. Amoretti *et al.*, Phys. Plasmas **10** 3056 (2003).
16. H. Higaki *et al.*, *Phys. Rev. E* **65**, 046410 (2002).
17. A. Speck *et al.*, *Phys. Lett. B* **650**, 119 (2007).
18. S. A. Prasad and T. M. O'Neil, *Phy. Fluids* **26**, 665 (1983).
19. G. N. Watson, *A Treatise on the Theory of Bessel functions*, (Cambridge U. Press, Cambridge, 1995).
20. J. K. Jennings, R. L. Spencer, and K. C. Hansen, *Phys. Plasmas* **2**, 2630 (1995).
21. L. Landau, *JETP* **15**, 574 (1946).
22. R. W. Gould, *Phys. Plasmas* **2**, 1404 (1995).